Electronic Supplementary Material (ESI) for Journal of Materials Chemistry C.
This journal is © The Royal Society of Chemistry 2024

Supporting Information

Low-temperature Open-atmosphere Growth of WO_3 Thin Films with Tunable and High-performance Photoresponse

Zhuotong Sun,[a] Subhajit Bhattacharjee,[b] Ming Xiao,[a,*,#] Weiwei Li,[c] Megan O. Hill,[a] Robert A. Jagt,[a] Louis-Vincent Delumeau,[d,e] Kevin P. Musselman,[d,e] Erwin Reisner,[b] and Judith L. MacManus-Driscoll[a,*]

[a]Department of Materials Science & Metallurgy, University of Cambridge, Cambridge, CB3 0FS, United Kingdom.

[b]Yusuf Hamied Department of Chemistry, University of Cambridge, Lensfield Road, Cambridge CB2 1EW, United Kingdom

[c]College of Physics, MIIT Key Laboratory of Aerospace Information Materials and Physics, Nanjing University of Aeronautics and Astronautics, Nanjing 211106, China

[d]Department of Mechanical and Mechatronics Engineering, University of Waterloo, Waterloo, Ontario N2L 3G1, Canada

[e]Waterloo Institute for Nanotechnology, Waterloo, Ontario N2L 3G1, Canada

[*]Corresponding Authors: Ming Xiao (xiaom37@mail.sysu.edu.cn) and Judith L. MacManus-Driscoll (jld35@cam.ac.uk)

[#]Present address: School of Microelectronics Science and Technology, Sun Yat-sen University, Zhuhai, 519082, Guangdong Province, China

Table S1. Parameters for the deposition of WO_3 film for the growth of WO3 thin film using AP-SCVD in this work.

PROCESS PARAMETER	PARAMETER RANGE
Ar carrier gas flow rate through precursor (sccm)	100-350
Substrate oscillation speed (mm/s)	10-90
Head-to-substrate spacing (µm)	200-1200
Oscillation cycles	100-3000
Deposition time (min)	3-60
Film thickness (nm)	10-200
Oxidant	H_2O, O_2, Air

Table S2. Summary of growth rate for different conditions as shown in Figure 2b.

Condition No.	Growth rate per cycle (g_c, nm/cycle)	Oscillation speed (mm/s)	Growth rate (nm/min)
1	0.135	10	5.4
2	0.027	50	5.4
3	0.068	10	2.7
4	0.015	90	5.4
5	0.0135	50	2.7
6	0.034	10	1.35
7	0.0075	90	2.7
8	0.00675	50	1.35
9	0.00375	90	1.35

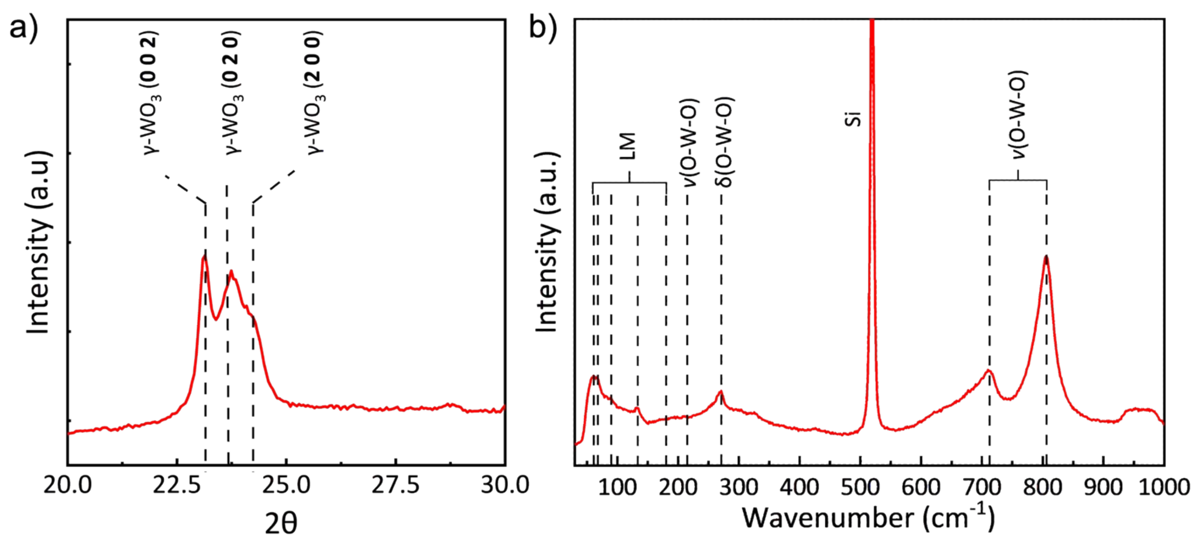

Figure S1. a) XRD pattern at 2θ from 20° to 30° of 200 nm film on SiO_2/Si substrate, b) Raman spectra for 200 nm film on SiO_2/Si substrate. LM indicates lattice mode. The peaks relating only to the WO_3 film are labeled O-W-O.

X-ray diffraction and Raman analysis were used to explore a 200 nm thick film, thick enough to obtain a sufficient signal. The film was deposited at 50 mm/s oscillation speed, 200 sccm gas flow rate through the precursor and 1000 µm spacing. Figure S1a shows a narrow part of an X-ray diffraction pattern from 20° to 30°, which shows the only peaks that are visible over a range of 10° to 80°. The three peaks observed at 23.1°, 23.6°, and 24.4°, correspond to the three most intense peaks of monoclinic WO_3, i.e. (0 0 2), (0 2 0), and (2 0 0) (JCPDS-01-083-0950). No other orientations were observed. Figure S2b shows the Raman spectrum of the same film, along with a bare SiO_2/Si substrate with the reference monoclinic WO_3 peaks shown in dashed lines.[1] Silicon peaks were observed at 301 cm^{-1}, 510 $cm^{-1,}$ and 950 cm^{-1}, with the peak at 510 cm^{-1} being a one-phonon peak and the broad peak at 950 cm^{-1} being the most intense two-phonon peak.[1] For WO_3, peaks are observed at 61 and 132 cm^{-1} (lattice modes of monoclinic WO_3), 270 cm^{-1} (bending mode of (O-W-O)), 325 cm^{-1} (stretching mode of (W-OH_2) from surface hydrates), 691 and 804

cm^{-1} (stretching modes of (O-W-O).[2] This result further confirms the monoclinic phase of the as-deposited WO_3 films.

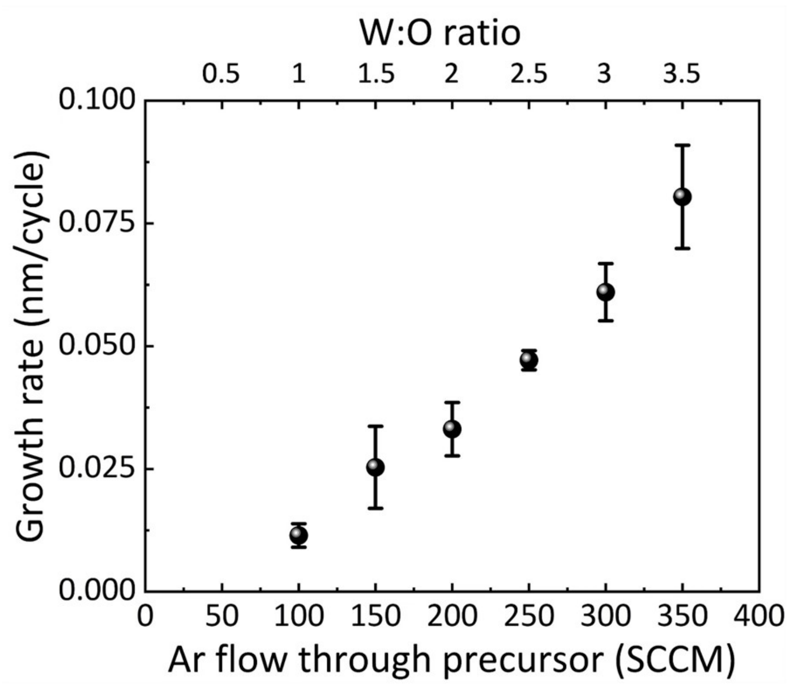

Figure S2. Effect of film thickness with the change of W:O ratio adapted from Figure 1 from the main text. It should be noted the oscillation speed remains at 50 mm/s in this case.

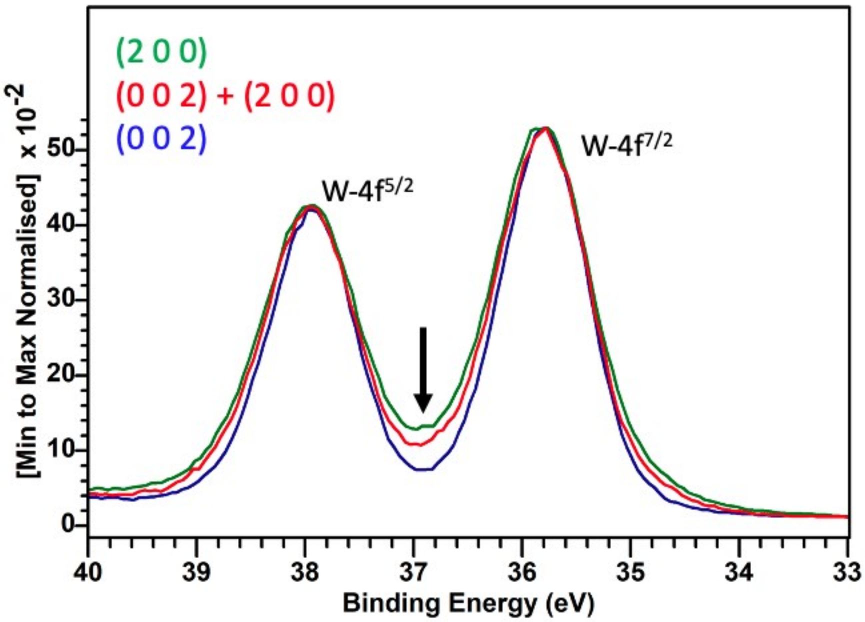

Figure S3. Overlay of normalized W-4f spectra of 30 nm (2 0 0) dominant, '(2 0 0) + (0 0 2)' mixture and (0 0 2) dominant WO_3 film.

Figure S3 shows the overlay of intensity normalized W-4f spectra for the samples from Figure 4c. The W-4f peaks are observed with approximately 2.14 eV splitting between W-4f$^{5/2}$ and W-4f$^{7/2}$ peaks. While the peak splitting remains constant between films, a variation in relative intensity between 4f$^{5/2}$ and 4f$^{7/2}$ is observed, marked by a black arrow. This suggests the presence of an additional component within the 4f spectra.

Additionally, Figure S4 compares XPS spectra from two films grown under the same growth conditions (condition 9). The film characterized in this work is shown on the left. Under condition 9, this film is (0 0 2) oriented and gives a W^{5+} atomic ratio of 0.9%. The second film grown for comparison under condition 9 is shown on the right. This film also shows an (0 0 2) orientation and gives a W^{5+} atomic ratio of 0.7%. This 0.2% difference in W^{5+} percent between the two films of the same condition shows that the concentration change between growth conditions (0.9%, 2.4%, and 3.2% for conditions 9, 5, and 1 respectively) is significant.

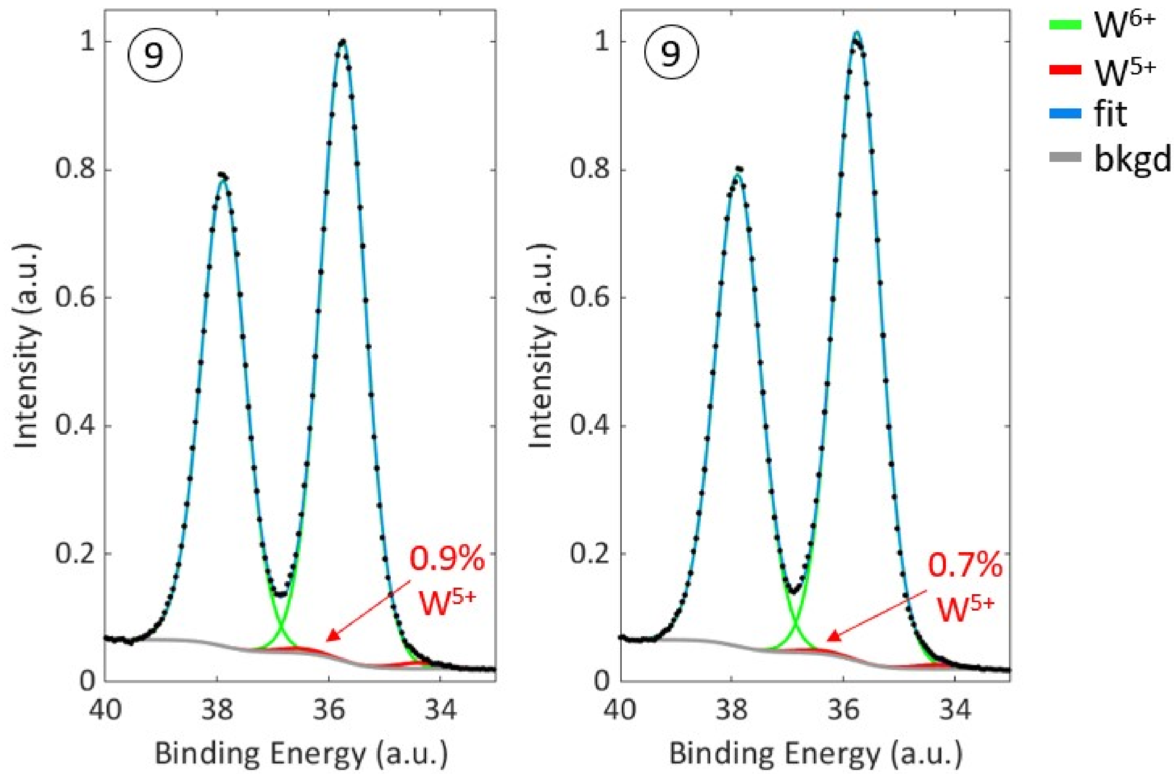

Figure S4. Comparison of XPS spectra from two films grown under the same growth conditions (condition 9). The film characterized in this work is shown on the left. The second film grown for comparison at condition 9 is shown on the right. Both films are (0 0 2) oriented.

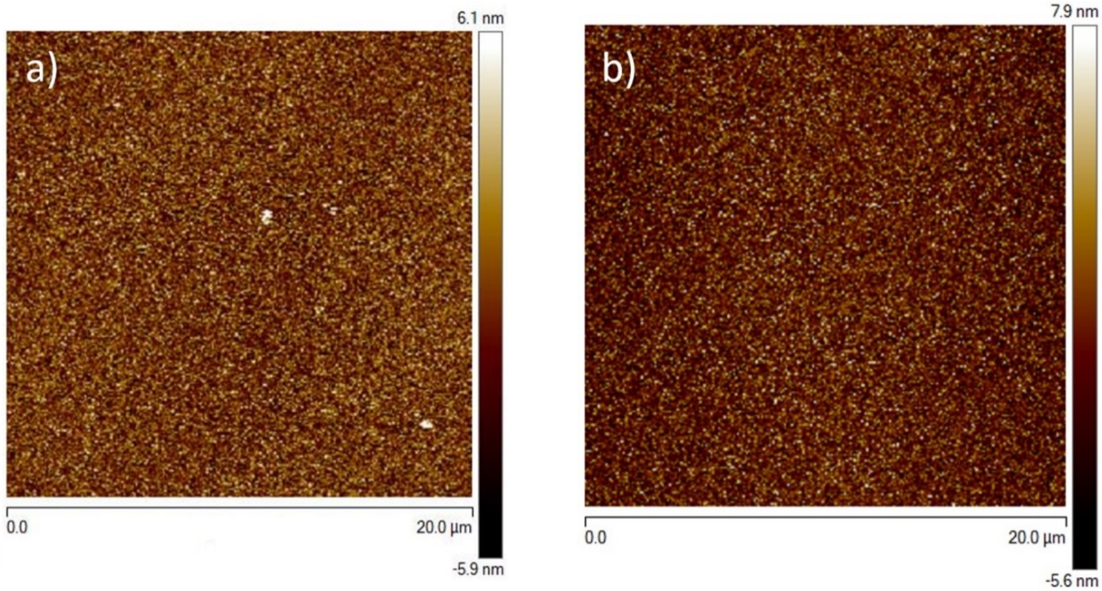

Figure S5. 20 µm × 20 µm AFM images of a) (2 0 0) dominant, and b) (0 0 2) dominant WO_3 films with 30 nm thickness

20 µm by 20 µm AFM images were taken to analyze the surface roughness of as-deposited WO_3 films. Figure S5a is the image of 30 nm (2 0 0) dominant orientation thin film and Figure S5b is an image of a 30 nm (0 0 2) dominant orientation thin film. NanoScope Analysis Software was used to analyze and obtain the film roughness.

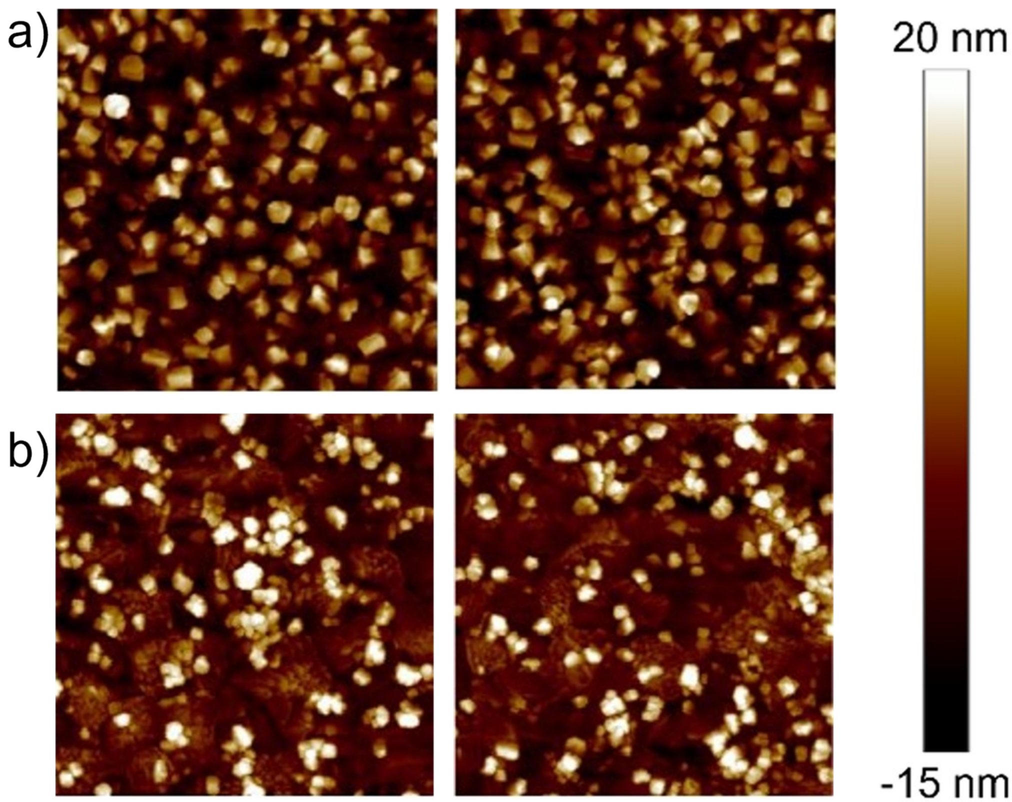

Figure S6. AFM characterization of surface morphology of WO_3 film at random locations on the Si substrates with the dominant orientation of a) (2 0 0) and b) (0 0 2), respectively. Consistent surface morphology over different locations on the Si substrate could be observed, confirming the uniformity of the as-deposited WO_3 film.

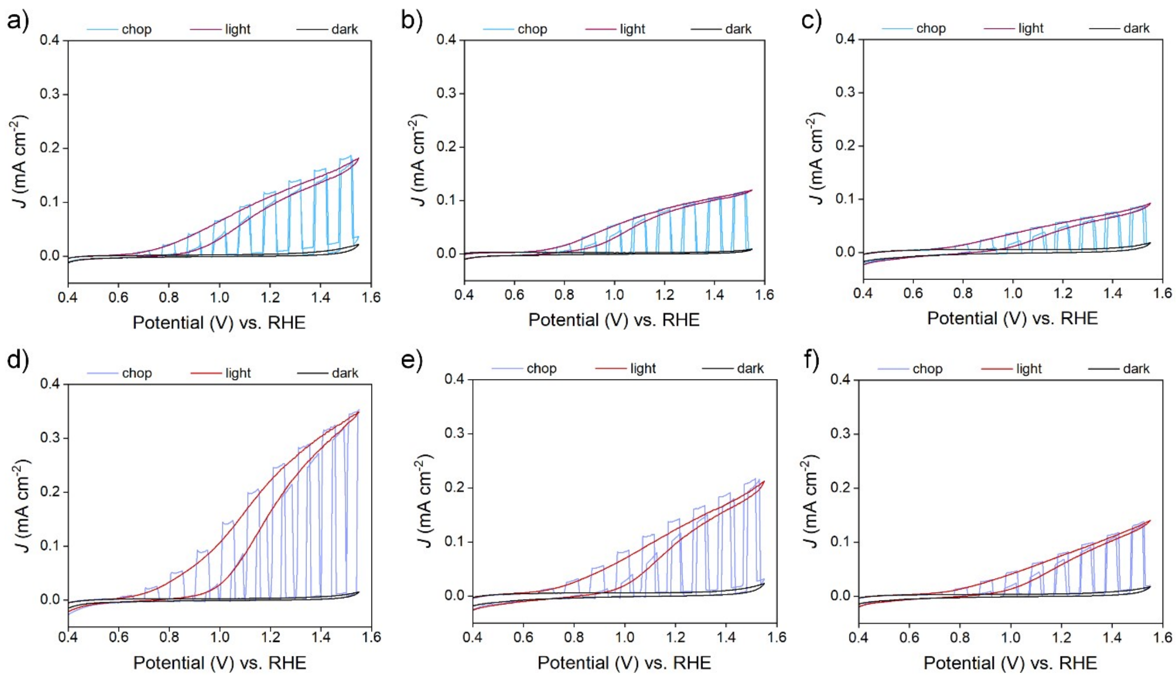

Figure S7. a-c) CV scans under chopped, continuous, and no artificial sunlight irradiation (1 sun) of the (a) WO_3-[002], (b) WO_3-[002]+[200] and (c) WO_3-[200] photoanodes. d-f) CV scans under chopped, continuous and no artificial concentrated sunlight irradiation (3 suns) of the (d) WO_3-[002], (e) WO_3-[002]+[200] and (f) WO_3-[200] photoanodes. Conditions: AM 1.5G, 0.5 M aqueous NaCl (pH ~6), room temperature.

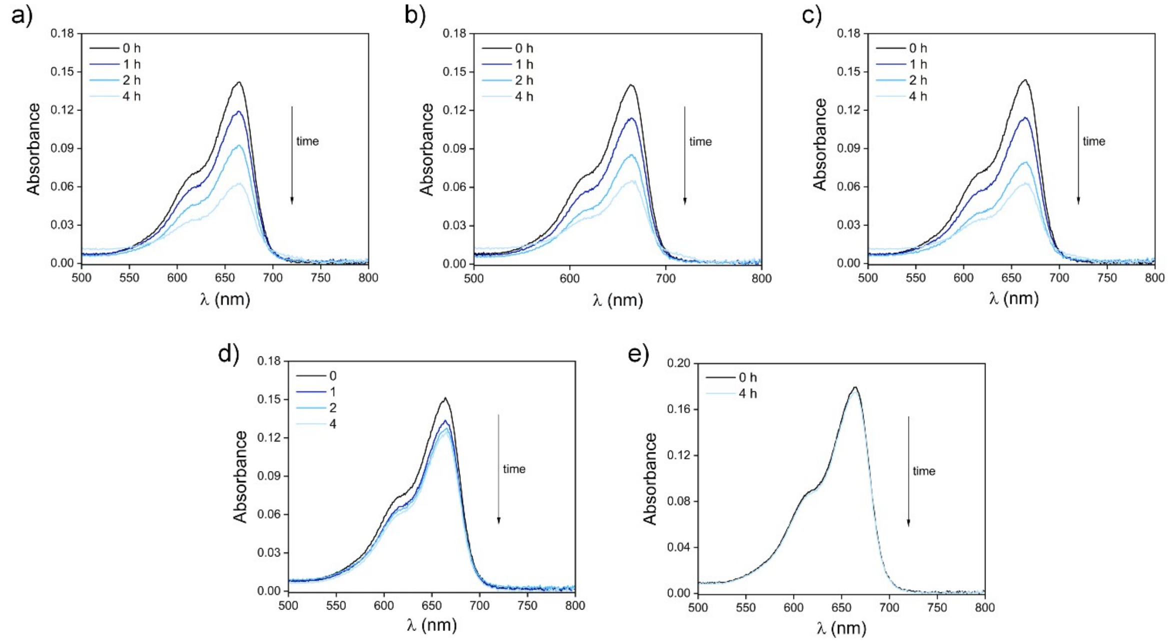

Figure S8. a-c) Absorption spectra of aqueous MB solution at different time intervals in presence of (a) WO_3-[002], (b) WO_3-[002]+[200], and (c) WO_3-[200] films under simulated sunlight (AM 1.5G, 1 sun). d-e) Control experiments in the absence of d) WO_3 film and e) light. The peak at ~664 nm is the characteristic peak of MB used for monitoring the degradation process.

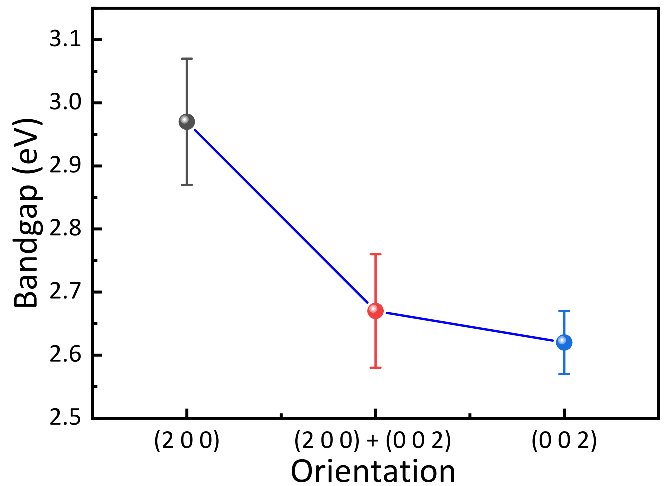

Figure S9. The band gap of 30 nm as-deposited WO_3 films on SiO_2/Si substrate with different orientations.

References

[1] K. Uchinokura, T. Sekine, E. Matsuura, Raman scattering by silicon *Solid State Commun.* **1972**, *11*, 47-49.

[2] M. F. Daniel, B. Desbat, J. C. Lassegues, B. Gerand, M. Figlarz, Infrared and Raman study of WO_3 tungsten trioxides and WO_3, xH_2O tungsten trioxide tydrates *J. Solid State Chem.* **1987**, *67*, 235-247.